



# Impact of Icebergs on Net Primary Productivity in the Southern Ocean

Shuang-Ye Wu<sup>1,2</sup>, Shugui Hou<sup>2</sup>

5 <sup>1</sup>Department of Geology, University of Dayton, Dayton, Ohio 45469, USA  
<sup>2</sup>School of Geographic and Oceanic Sciences, Nanjing University, Nanjing 210093

Correspondence to: Shuang-Ye Wu ([swu001@udayton.edu](mailto:swu001@udayton.edu)), Shugui Hou ([shugui@nju.edu.cn](mailto:shugui@nju.edu.cn))

**Abstract.** Productivity in the Southern Ocean (SO) is iron-limited, and supply of iron dissolved from aeolian dust is believed to be the main source from outside the marine environment. However, recent studies show that icebergs could provide comparable amount of bioavailable iron to the SO as aeolian dust. In addition, small scale areal studies suggest increased concentrations of chlorophyll, krill, and seabirds surrounding icebergs. Based on previous research, this study aims to examine whether iceberg occurrence has a significant impact on marine productivity for the entire SO (south of 40° S), using remote sensing data of monthly iceberg amount and monthly ocean net primary productivity (NPP) covering the period 2002-2014. Using global and geographically weighted multiple linear regression models, and controlling for temperature, our analyses show that iceberg presence has a small, yet statistically significant, positive impact on the SO NPP. NPP in the SO is largely influenced by temperature, which could explain 43% of the total variance in NPP with the standardized coefficient of 0.68. However, in places with iceberg presence, temperature influence weakens, indicated by lower partial temperature  $R^2$  (0.19) and standardized coefficient (0.45). Meanwhile, iceberg probability could independently explain 2% of the NPP variance with a standardized coefficient of 0.15. Although small, this influence is statistically significant at 0.01 level. The geographically weighted regression model reveals spatial variation of these relationships. The results suggest that as iceberg quantity increases, their positive influence on NPP also increases, as indicated by increasing iceberg partial  $R^2$  and standardized coefficient in the models.

## 1 Introduction

Iron, the fourth most abundant crustal element, has received widespread attention since the late 1980s due to its particular relevance for biogeochemical cycles in the ocean, especially in the high-nutrient low chlorophyll (HNLC) oceanic areas where plenty of macro-nutrients, such as nitrate and phosphate, are present, but with limited Fe (Falkowski et al., 1998). Changes in iron supply to oceanic planktons are thought to have a significant effect on concentrations of atmospheric carbon dioxide by altering rates of carbon sequestration, a theory known as the ‘iron hypothesis’ (Martin, 1990). The iron hypothesis stimulated new interests into the iron-enrichment experiments ranging from microcosmic (e.g. de Baar et al., 1990) to large scale studies (e.g. de Baar et al., 2005) in either natural or artificial settings. These studies have demonstrated that Fe serves as a major control over both the primary productivity and the planktonic community structure in HNLC waters



in more than 25% of the world oceans. Fe can take different forms in the oceans, e.g. particulate, colloidal, soluble, and as inorganic or organic complexes. The concentration of total dissolved Fe is generally low in SO water. De Baar and de Jong (2001) estimate it between 0.1–0.6 nmol L<sup>-1</sup>. This is often not sufficient to sustain the planktonic growth hence limits the primary productivity of the ocean (Price and Morel, 1998). The wide SO area is a place for intermediate- and deep-water formation, as well as the largest repository of unused macronutrients in surface waters. As a result, it is a potential site for enhanced sequestration of carbon (Cooper et al., 1996) if extra Fe could be supplied to promote plankton growth. It is suggested that this is the primary reason for the SO CO<sub>2</sub> ‘leak’ to be stemmed during ice ages, increasing ocean CO<sub>2</sub> storage and thus lower atmospheric CO<sub>2</sub> concentration (Sigman et al., 2000).

Cassar et al. (2007) summarized five sources of bioavailable iron to the SO surface waters, i.e., melting of sea ice, the release of dissolved iron or resuspension of sediments, upwelling supplies iron, vertical mixing supplies iron, and delivery of soluble iron by aerosol deposition supplies. They further confirmed that aerosol iron deposition has a significant influence on variability of net community production (NCP), as well as gross primary production (GPP) over the large SO areas. The first global maps of aerosol iron flux to the ocean were based on aerosol sampling networks, such as the SEAREX (Duce and Tindale, 1991). These maps revealed that the SO waters are characterized by particularly low aerosol iron fluxes. Particles in ice can be transported by icebergs from coastal regions into SO, releasing bioavailable Fe to the open water during melting along the tracks. Thus icebergs in the SO waters have also been shown to transport nutrients, together with bioavailable Fe, which could have a significant impact on ocean primary productivity (Raiswell et al., 2008; Lancelot et al., 2009; Schwarz and Schodlok, 2009). Raiswell et al. (2008) demonstrated the presence of potentially bioavailable Fe as ferrihydrite and goethite in nanoparticulate clusters, and estimated comparable fluxes of bioavailable iron supplied to SO from icebergs (0.06–0.12 Tg yr<sup>-1</sup>) and aerosol deposition (0.01–0.13 Tg yr<sup>-1</sup>). Raiswell and Canfield (2012) recently even suggested that icebergs could supply more than 90% of total colloidal and filterable Fe in the SO. Duprat et al. (2016) studied the influence of giant icebergs, over 18 km in length, on marine primary production in the SO, and detected substantially enhanced chlorophyll levels, typically over a radius of at least 4–10 times the iceberg’s length, that can persist for more than a month following passage of a giant iceberg. Therefore, an increase in the SO carbon sequestration through enhanced marine productivity due to fertilization by giant icebergs may become more important with future warming.

Despite the great interests and several small scale areal studies suggesting increased concentrations of chlorophyll, krill, and seabirds surrounding icebergs, there seems to be a lack of large-scale studies that examine the impact of iron on total productivity in SO. The distribution of ice volume, with its strong seasonal cycle, shows very high spatial and temporal variability, which is much contrasted in the three ocean basins (South Atlantic, Indian and Pacific oceans). Therefore, this study aims to examine such variability of iceberg occurrence and whether it has a significant impact on marine productivity for the entire SO (south of 40° S), using remote sensing data of monthly iceberg amount and monthly ocean NPP covering the period 2002-2014. Most previous work focus on large icebergs. However Tournadre et al. (2012) show that a majority of small icebergs are directly associated with the large ones. Therefore, the study of total iceberg occurrence should reveal similar impacts on ocean productivity.



## 2 Data and methodology

### 2.1 Data

Three major datasets are used in this study. First, monthly ocean NPP ( $\text{mg C m}^{-2} \text{ day}^{-1}$ ) data is obtained from Oregon State University Ocean Productivity website (<http://www.science.oregonstate.edu/ocean.productivity/index.php>) and covers the years 2002-2014. The data is derived from MODIS R2013.1 data using the Vertically Generalized Production Model (VGPM) (Behrenfeld and Falkowski, 1997) as the standard algorithm. In this model, NPP is a function of chlorophyll, available light, and the photosynthetic efficiency. This is a global dataset with a spatial resolution of 0.167 degrees. Second, monthly iceberg data is obtained from Iceberg Database of the Merged Altimeter for Altiberg project (<ftp://ftp.ifremer.fr/ifremer/cersat/projects/altiberg/>) for 1992-2014. The data is generated based on remote sensing techniques developed by Tournadre et al. (2012). The data contains three variables: iceberg presence probability, surface area and volume. For most of the analysis we made use of iceberg probability of presence, which is defined in Tournadre et al. (2012) as “the ratio of the number of icebergs detected within a grid cell by the total number of valid satellite data samples within the same grid cell”. Iceberg surface area and volume are correlated to iceberg probability but their estimation introduces greater uncertainties and are therefore not used. The dataset covers the entire SO (south of  $40^\circ \text{ S}$ ) at a spatial resolution of 1 degree. Finally, monthly air temperature is obtained from EAR-Interim reanalysis data for 1979-2014 (<http://apps.ecmwf.int/datasets/>) at a spatial resolution of 0.7 degree. We extracted all data for the period 2002-2014 for area south of  $40^\circ \text{ S}$ , and resampled them to a common grid of  $1 \times 1$  degree.

### 2.2 Methodology

Multiple linear regression (MLR) is the major tool to examine the effect of temperature and iceberg concentration on the SO NPP. The general model is specified as follows:

$$\log(NPP) = \beta_0 + \beta_1 * T + \beta_2 * P$$

where  $T$  is air temperature and  $P$  is iceberg probability. Log transformation is performed for NPP because the model residuals are largely positively skewed with the original data. The model is fitted in two ways. First, a global regression model is developed by using all temporal and spatial data within the study area to estimate the model parameters. A global model defines a single relationship that applies throughout the study area. However this relationship between NPP,  $T$  and  $P$  may not be spatially stationary. Therefore, we also apply a geographically weighted regression (GWR) model to examine how this relationship varies over our study domain. We first select a fixed bandwidth around each data grid point by cross-validation. We then use all the data within the bandwidth, both spatial and temporal data, weighted by a Gaussian kernel to fit the same model. Standard t-test and F-test are used to evaluate the statistical significance of the coefficients and the models.



The relative influence of temperature and iceberg presence on NPP is examined in three different ways. First, we examine the correlation between NPP and each of the two independent variables (T and P) individually through the use of both complete and partial correlation analysis. Partial correlation is a measure of the strength and direction of a linear relationship between two continuous variables (e.g. NPP and P) whilst controlling for the effect of one or more other continuous variables (e.g. T). In both analyses, Pearson's  $r$  is used as the measure of correlation. Second, we standardize all variables in the following way:

$$z = \frac{x - \mu}{\sigma}$$

where  $z$  is the standard z-score of the variable,  $x$  is the original variable,  $\mu$  is the mean of the variable and  $\sigma$  is the standard deviation of the variable. After fitting the regression model as outlined above, standardized coefficients are used to indicate the expected increase or decrease in *NPP*, in standard deviation units, given a one standard deviation increase in the explanatory variable (*T* or *P*). Finally, relative weights are used to examine how much of the variance in the NPP can be explained independently by the variance of each of the explanatory variables (*T* or *P*). Relative weight analysis is a method for partitioning the independent contribution from each explanatory variable (*T* or *P*) to the total  $R^2$  of the MLR model (Johnson, 2000). When these variables are uncorrelated, the relative weights are simply computed as the squared correlation coefficient between each explanatory variable and the dependent variable. The sum of these relative weights should be equal to the model  $R^2$ . When they are correlated, principal components analysis is used to transform the original explanatory variables into a set of uncorrelated principal components (PCs). These PCs are then submitted to two correlation analyses. The first is the correlation between the dependent variable and the uncorrelated PCs. The second is the correlation between the original explanatory variables and the uncorrelated PCs. Relative weights are computed by multiplying squared correlation coefficients from the first analysis with squared correlation coefficients from the second analysis. The relative weights measure the independent contributions of each explanatory variable to the total model  $R^2$ , i.e. the amount variance in the dependent variable that could be explained by the model. The sum of all relative weights equals to the model  $R^2$ .

### 3 Results

#### 3.1 Spatial distribution of NPP and iceberg concentration

Figure 1 shows the spatial distribution of NPP (Fig. 1a) and iceberg probability (Fig. 1b) in the SO. Figure 2 summarizes the latitudinal distribution of mean NPP and iceberg probability. NPP is relatively high near the coast of Antarctica, largely because of nutrient input from the continent. It then steadily decreases into a zone of very low values, reaching the minimum around  $-60^\circ$  S. It then increases with latitudes, influenced by the increasing temperature and other factors. Longitudinally, icebergs concentration has three high value regions, one in each ocean. These are caused by general iceberg circulation pattern in the SO (Tournadre, 2012; Gladstone et al., 2001). The largest of these high concentration regions is located at southern Atlantic Ocean north of the Wendell Sea. Latitudinally, icebergs concentrate in a zone between  $-75^\circ$  to  $-65^\circ$  S just



off the coast of Antarctica, peaking around  $-70^{\circ}$  S. It partly overlaps with the zone of relative low NPP in the SO from  $-70^{\circ}$  S to  $-50^{\circ}$  S. It then gradually decreases until its northern limit at about  $-50^{\circ}$  S.

### 3.2 Temporal trends of NPP and iceberg concentration

Figure 3 shows the time series of monthly NPP (Fig. 3a) and total iceberg volume (Fig. 3b) covering the years 2002-2012. The data is both presented as the SO total, and separated into three sections: the southern Atlantic (from  $70^{\circ}$  W to  $30^{\circ}$  E), the southern Indian (from  $30^{\circ}$  E to  $150^{\circ}$  E), and the southern Pacific (from  $150^{\circ}$  E to  $70^{\circ}$  W). Both NPP and iceberg volume show regular seasonal cycles with high values in the austral summer and low values in the austral winter. This is largely controlled by the temperature variation. Despite these seasonal variations, NPP in the SO shows no significant trends over the study period. The iceberg concentration shows regular seasonal changes as well as inter-annual variations. The total iceberg volume seems to be decreasing slightly in the S. Atlantic, and increasing slightly in the S. Pacific and S. Indian Oceans. However, owing the shortness of records, none of the trends has statistical significance.

### 3.3 Correlation between monthly NPP and temperature, iceberg probability

Global correlation analysis is conducted using the pooled monthly data at all grid cells within the study area. We first calculate the Pearson's correlation coefficient for NPP and temperature, NPP and iceberg probability, respectively. In addition, we calculate the partial correlation coefficient between NPP and temperature controlling for iceberg probability, and that between NPP and iceberg probability controlling for temperature. We repeat these analyses for pooled monthly data at grid cells with iceberg presence. Results are presented in Table 1. Correlation analysis shows that for all grid cells, NPP is significantly correlated with temperature ( $r = 0.66$ ), but not with iceberg probability ( $r = -0.03$ ). However, if only the cells with iceberg presence are considered, NPP becomes significantly correlated with iceberg probability ( $r = 0.12$ ), whereas the correlation between NPP and temperature greatly weakens ( $r = 0.27$ ) albeit still significant. When temperature is controlled, the correlation between NPP and iceberg probability increases significantly both in case of all grid cells and for cells with iceberg presence. In all cases, NPP is positively correlated with iceberg probability, suggesting that the presence of iceberg tends to increase NPP in those places.

In order to examine the spatial variation of these relationships, we perform correlation analysis at each grid cell using the monthly data between NPP and temperature, and between NPP and iceberg probability, respectively. The results are presented in Fig. 4a and 4b. The correlation between NPP and temperature is strongest in places with no or little iceberg presence, e.g. at lower latitudes and closer to the Antarctic coast. In the zone where icebergs concentrate ( $-75^{\circ}$  to  $-65^{\circ}$  S), the correlation is much weaker for NPP and temperature (Fig. 4a). The correlation between NPP and iceberg probability is highest at those places with high concentration of icebergs (Fig. 4b).



### 3.4 Contribution of iceberg concentration on NPP based on regression analysis

Global regression uses all data in the study area to fit a single MLR model. We first established a global MLR model for data from all grid cells, and one for data from cells with iceberg presence only. We use relative weights to partition the model  $R^2$  between the explanatory variables (T and P), and calculate their standardized coefficients to examine their respective influence on NPP. The results are presented in Table 2. For all grid cells, the model could explain 44% of the variance in NPP, however most of the variance is explained by temperature (43%). The standardized coefficients also confirm the dominant effect of temperature on NPP (0.68 for T vs. 0.1 for P). Iceberg probability has very little influence on NPP, with small  $R^2$  and coefficient that is not statistically significant. When the regression model is fitted to only cells with iceberg presence, the total model  $R^2$  decreases (0.21). However, the effect of the iceberg probability on NPP increases as measured by both  $R^2$  (0.02) and standardized coefficient (0.15). This effect is statistically significant at critical level of 0.01.

Geographically weighted regression (GWR) fits a model at each grid cell using all the data within a defined neighbourhood. This allows us to examine the spatial variation of the contribution from the two explanatory variables. Since it requires data from both variables, GWR is only performed over grid cells with iceberg presence. The partition of  $R^2$  between temperature and iceberg probability is presented in Fig. 5. It largely confirms the previous result, showing that temperature has greater influence on NPP in places with low iceberg presence, and that its impact weakens in places with high iceberg concentration (Fig. 5a). On the other hand, iceberg probability has the strongest impact on NPP, as measured by its partial  $R^2$ , in places with high iceberg concentration (Fig. 5b). We further break all grid cells into 4 equal-sized groups based on increasing iceberg occupancy, and examined the model results within each group (Table 3). It can be seen that as iceberg occupancy increases, the part of the NPP variance that could be explained by P also increases, as does the impact of P on NPP as indicated by the standardized coefficients.

## 4 Discussion and conclusion

In this study, we aim to examine whether iceberg occurrence has a significant impact on marine productivity for the entire SO (south of 40° S), using remote sensing data of monthly iceberg amount and monthly ocean NPP covering the period 2002-2014. Using global and geographically weighted multiple linear regression models, and controlling for temperature, our analyses show that iceberg presence has a small, yet statistically significant, positive impact on the SO NPP. NPP in the SO is largely influenced by temperature, which could explain 43% of the total variance in NPP with the standardized coefficient of 0.68. However, in places with iceberg presence, temperature influence weakens, indicated by lower partial temperature  $R^2$  (0.19) and standardized coefficient (0.45) in the regression model. Meanwhile, in places with iceberg presence, iceberg probability could independently explain 2% of the NPP variance with a standardized coefficient of 0.15. Although small, this influence is statistically significant at 0.01 level. The result is not surprising for several reasons. The direct correlation between NPP and iceberg amount could be weakened by other sources of Fe (such as meltwater, sedimentary, and upwelling sources), variable phytoplankton Fe:C quotas, light and silicate limitations, the atmospheric Fe



dissolution kinetics, aeolian Fe sources and transport pathways. In addition, the statistical relationship between SO NPP and iceberg amount also depends on the forms of Fe in icebergs. Most previous studies focus on direct measurement of soluble iron. However, Hassler and Schoemann (2009) found no direction link between soluble and bioavailable Fe because organic ligands have the differential effects on the solubility and the bioavailability. Several studies seem to suggest that organic colloidal Fe provides an important pool to sustain Fe bioavailability to phytoplankton (e.g. Nodwell and Price, 2001; Chen et al., 2003; Wang and Dei, 2003). Finally, icebergs themselves could have other effects on NPP. For example, Arrigo and van Dijken (2004) observed that icebergs could have negative effects on the polar marine ecosystems. Many of these icebergs have long residence times, and hence are likely to have been located in highly productive coastal waters during the peak growing seasons of spring and summer. Their presence can alter normal advection patterns of annual sea-ice, and hence the fraction of open water available for phytoplankton growth. All these factors could have contributed to a relatively weak correlation between SO NPP and iceberg occurrences. For more detailed studies on the impact of icebergs relative to some of the factors listed above, we need to develop quantifiable indicators for these factors and incorporate them into statistical modelling. Such indicators could include distance to the coast, distance to aeolian dust sources along transport pathways based on atmospheric circulation patterns, proportions of bioavailable iron to total soluble iron from iceberg case studies, ocean circulation patterns etc.

The geographically weighted regression model in this study reveals spatial variation of the relationship between NPP and iceberg presence. The results suggest that in places with increasing number of icebergs, their positive influence on NPP also increases, as indicated by increasing iceberg partial  $R^2$  and standardized coefficient in the models. This seem to suggest that with global warming, it is possible that growing iceberg quantity could increase their positive impact on the SO NPP, hence serving as a negative feedback to the climate system by increasing carbon sequestration in the SO.

### Acknowledgement

The research was supported by the State Oceanic Administration (CHINARE2012-02-02) and the Natural Science Foundation of China (41330526, 41171052, 41321062, and 41571180).

### References

- Behrenfeld, M. J. and Falkowski, P. G.: Photosynthetic rates derived from satellite-based chlorophyll concentration, *Limnol. Oceanogr.*, 42(1), 1-20, 1997.
- Cassar, N., Bender, M. L., Barnett, B. A., Fan, S., Moxim, W. J., Levy II, H. and Tilbrook, B.: The Southern Ocean biological response to aeolian Iron deposition, *Science*, 317, 1067-1070, doi: 10.1126/science.1144602, 2007.
- Cooper, D. J., Watson, A. J. and Nightingale, P. D.: Large decrease in ocean-surface CO<sub>2</sub> fugacity in response to in situ iron fertilization, *Nature*, 383, 511–513, 1996.





- de Baar, H. J. W., Buma, A. G. J., Nolting, R. F., Cadée, G. C., Jacques, G. and Treguer, P. J.: On iron limitation of the Southern Ocean: experimental observations in the Weddell and Scotia Seas, *Mar. Ecol. Prog. Ser.*, 65, 105–122, 1990.
- de Baar, H. J. W. and de Jong, J. T. M.: Distribution, sources and sinks of iron in seawater, in *The Biogeochemistry of Iron in Seawater*, edited by: Turner, D. R. and Hunter, K. H., IUPAC Series on Analytical and Physical Chemistry of Environmental Systems, vol. 7, Wiley, New York, 123–153, 2001.
- de Baar, H. J. W., Boyd, P. W., Coale, K. H., Landry, M. R., Tsuda, A., Assmy, P., Bakker, D. C. E., Bozec, Y., Barber, R. T., Brzezinski, M. A., Buesseler, K. O., Boye, M., Croot, P. L., Gervais, F., Gorbunov, M. Y., Harrison, P. J., Hiscock, W. T., Laan, P., Lancelot, C., Law, C. S., Lvasseur, M., Marchetti, A., Millero, F. J., Nishioka, J., Nojiri, Y., van Oijen, T., Riebesell, U., Rijkenberg, M. J. A., Saito, H., Takeda, S., Timmermans, K. R., Veldhuis, M. J.W., Waite, A. M. and Wong, C.-S.: Synthesis of iron fertilization experiments: from the iron age in the age of enlightenment, *J. Geophys. Res.*, 110, C09S16/01–C09S16/24, doi:10.1029/2004JC002601, 2005.
- Duce, R. A. and Tindale, N. W.: Atmospheric transport of iron and its deposition in the ocean, *Limnol. Oceanogr.*, 36, 1715–1726, 1991.
- Duprat, L. P. A., Bigg, G. R., David J. and Wilton, D. J.: Enhanced Southern Ocean marine productivity due to fertilization by giant icebergs, *Nature Geo.*, doi: 10.1038/NGEO2633, 2016.
- Falkowski, P. G., Barber, R. T. and Smetacek, V.: Biogeochemical controls and feedbacks on ocean primary production, *Science*, 281, 200–206, 1998.
- Gladstone, R. M., Bigg, G. R. and Nicholls, K. W.: Iceberg trajectory modeling and meltwater injection in the Southern Ocean, *J. Geophys. Res.*, 106(C9), 19903–19915, 2001.
- Johnson, J. W.: A heuristic method for estimating the relative weight of predictor variables in multiple regression, *Multivariate Behavioral Res.*, 35(1), 1–19, 2000.
- Lancelot, C., de Montety, A., Goosse, H., Becquevort, S., Schoemann, V., Pasquer, B. and Vancoppenolle, M.: Spatial distribution of the iron supply to phytoplankton in the Southern Ocean: a model study, *Biogeosciences*, 6, 2861–2878, 2009.
- Martin, J. H.: Glacial-interglacial CO<sub>2</sub> change: the iron hypothesis, *Paleoceanography*, 5, 1–13, 1990.
- Price, N. M. and Morel, F. M. M.: Biological cycling of iron in the ocean, *Met. Ions Biol. Syst.*, 35, 1–36, 1998.
- Raiswell, R., Benning, L. G., Tranter, M. and Tulaczyk, S.: Bioavailable iron in the Southern Ocean: the significance of the iceberg conveyor belt, *Geochem. Trans.*, 9, 1–23, doi:10.1186/1467-4866-9-7, 2008.
- Raiswell, R. and Canfield, D.: The iron biogeochemical cycle past and present, *Geochem. Perspec.*, 1(1), 1–220, 2012.
- Schwarz, J. N. and Schodlok, M. P.: Impact of drifting icebergs on surface phytoplankton biomass in the Southern Ocean: ocean colour remote sensing and in situ iceberg tracking, *Deep Sea Res., Part I*, 56(10), 1727–1741, doi:10.1016/j.dsr.2009.05.003, 2009.





Sigman, D. M., Hain, M. P. and Haug, G. H.: The polar ocean and glacial cycles in atmospheric CO<sub>2</sub> concentration, *Nature*, 466, 47-55, doi:10.1038/nature09149, 2000.

Tournadre, J., Girard-Ardhuin, F. and Legrésy, B.: Antarctic icebergs distributions, 2002–2010, *J. Geophys. Res.*, 117, C05004, doi:10.1029/2011JC007441, 2012.



## Tables

**Table 1. Correlation between NPP and iceberg probability (P) and temperature (T)**

	Correlation		Partial Correlation	
	P	T	P	T
All cells	-0.03	0.66*	0.13*	0.66*
Cells with icebergs	0.12*	0.27*	0.17*	0.29*

\*Statistically significant at 0.01.

5

**Table 2. Global regression model results**

	R-squared			standardized coefficient	
	P	T	Total	P	T
All cells	0.006	0.43	0.44*	0.1	0.68*
Cells with icebergs	0.02	0.19	0.21*	0.15*	0.45*

\*Statistically significant at 0.01

**Table 3. Geographically weighted regression results**

Iceberg Occupancy	% of observation with icebergs	R-squared			standardized coefficient	
		P	T	Total	P	T
Quarter 1	3	0.004	0.35	0.36*	0.038	0.59*
Quarter 2	12	0.014	0.24	0.25*	0.081*	0.47*
Quarter 3	27	0.0245	0.22	0.25*	0.083*	0.45*
Quarter 4	48	0.0249	0.2	0.23*	0.076*	0.44*
Total	23	0.02	0.26	0.28*	0.07*	0.49*

\*Statistically significant at 0.01

10



## Figures

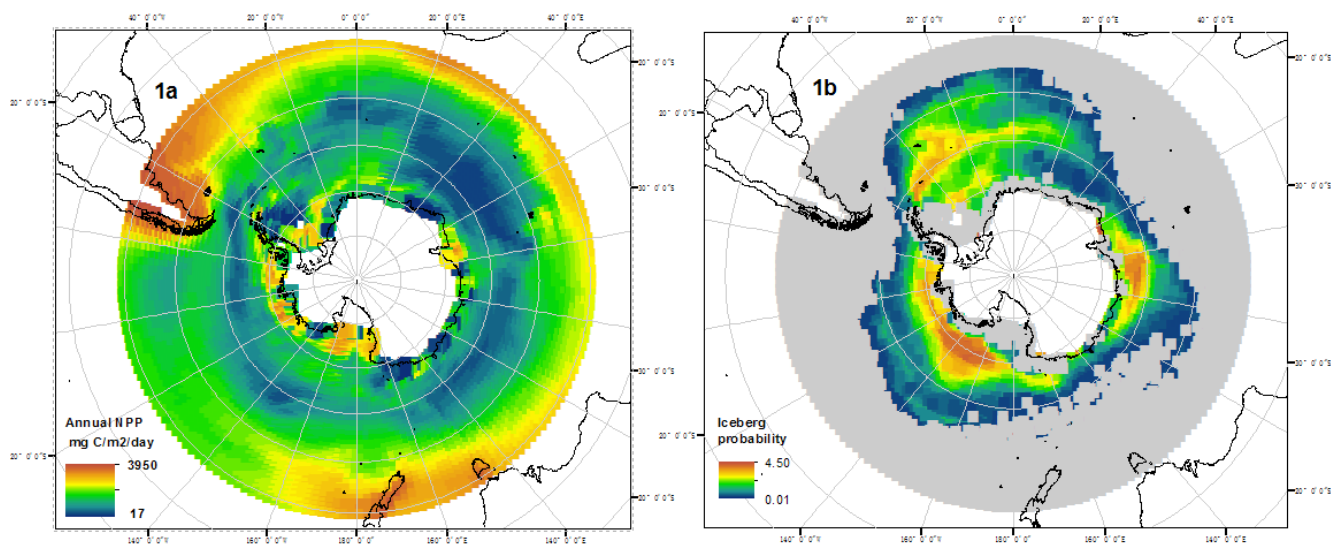
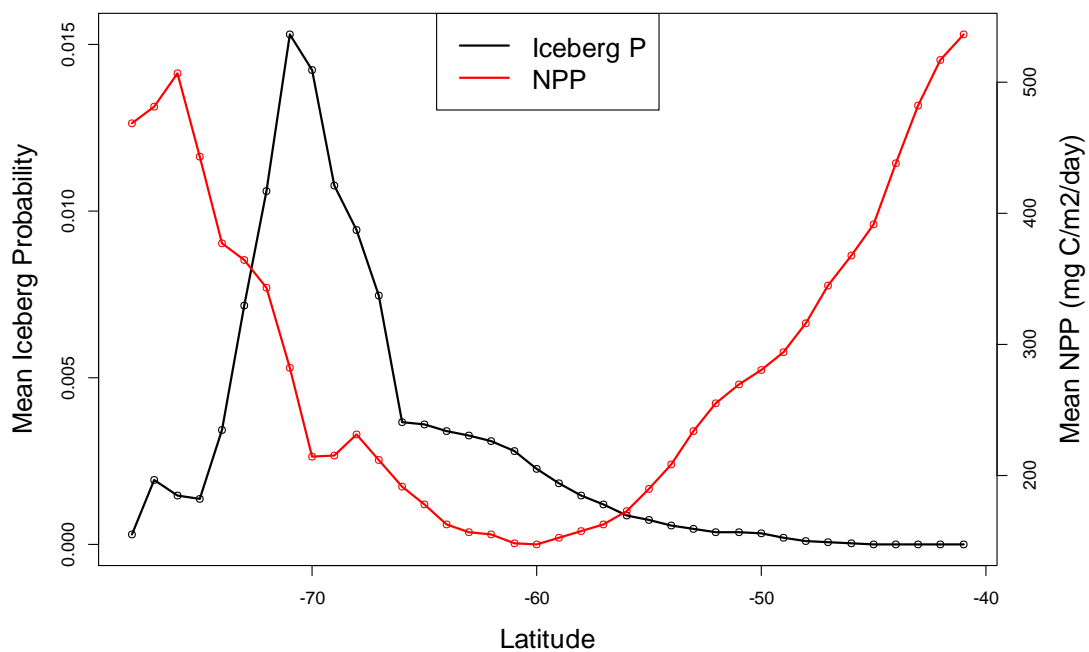
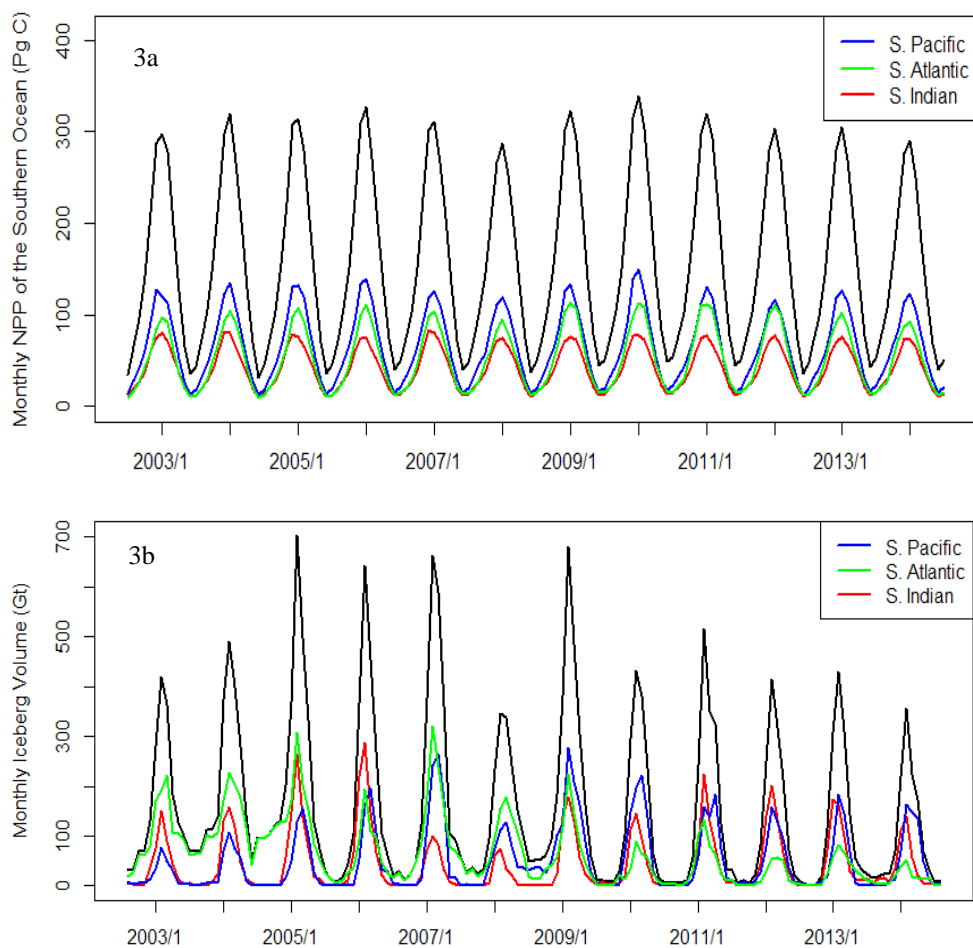


Fig. 1. Spatial distribution of ocean NPP (1a) and iceberg probability (1b).



5 Fig. 2. Latitudinal distribution of ocean NPP and iceberg probability.



**Fig. 3.** Temporal trends of NPP (3a) and iceberg volume (3b).

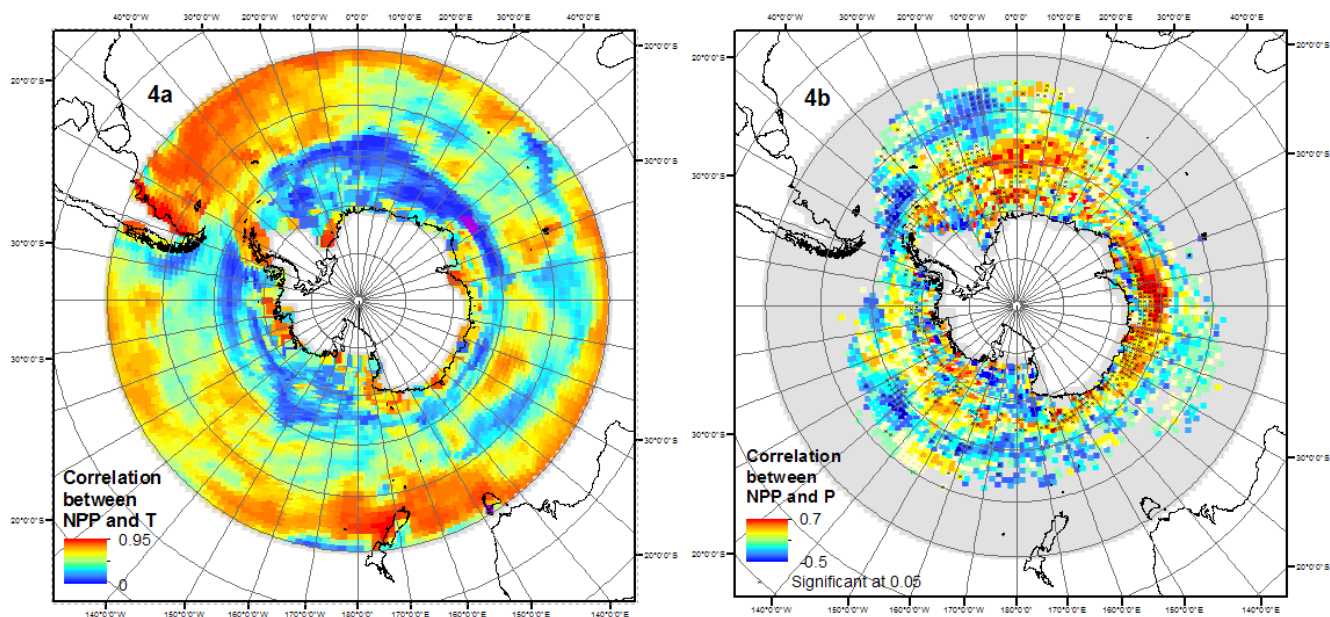
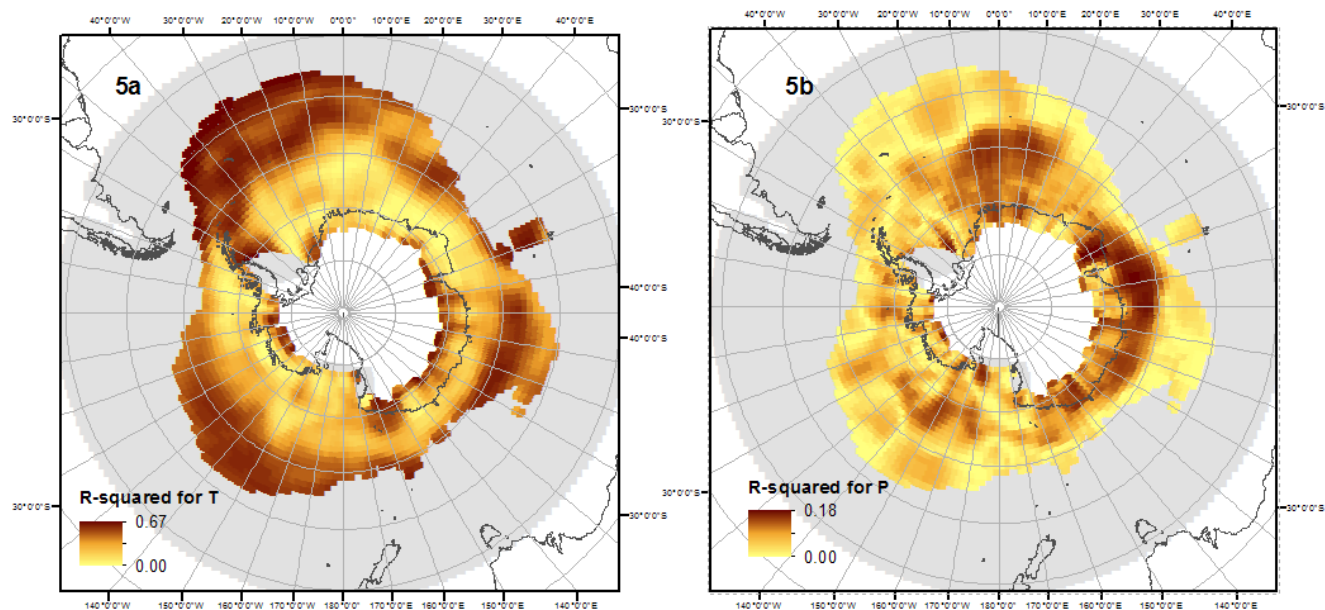


Fig. 4. Temporal correlation between monthly NPP and temperature (4a); between NPP and iceberg probability (4b).



5

Fig. 5. Partial  $R^2$  for temperature (5a) and iceberg concentration (5b) for geographically weighted regression model.